



# Bi<sub>2</sub>O<sub>3</sub> modified cobalt hydroxide as an electrode for alkaline batteries

T.N. Ramesh\*, P. Vishnu Kamath

Department of Chemistry, Central College, Bangalore University, Bangalore 560001, India

Received 13 January 2008; accepted 30 January 2008

Available online 12 February 2008

## Abstract

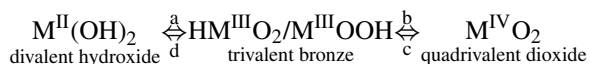
Manganese dioxide electrode shows reversible charge storage capacity, if the charge–discharge process is limited to 0.3e<sup>−</sup> exchange. Addition of small amount of Bi<sub>2</sub>O<sub>3</sub> to manganese dioxide induces reversibility with an exchange of 2e<sup>−</sup>/Mn. Nickel hydroxide is known to reversibly exchange 1e<sup>−</sup>. In spite of isostructural relationship between the cobalt hydroxide, nickel hydroxide and manganese dioxide, cobalt hydroxide does not show any electrochemical activity. Bi<sub>2</sub>O<sub>3</sub> modified cobalt hydroxide electrodes exchanges 0.3–0.5e<sup>−</sup>/Co during the charge discharge process. The oxidation–reduction process in cobalt hydroxide and Bi<sub>2</sub>O<sub>3</sub> modified cobalt hydroxide electrodes were monitored using the PXRD patterns. © 2008 Elsevier Ltd. All rights reserved.

**Keywords:** Cobalt hydroxide; Bi<sub>2</sub>O<sub>3</sub>; Electrode material; Alkaline batteries

## 1. Introduction

Transition metal oxides and hydroxides such as manganese dioxide and nickel hydroxide are extensively used as positive electrode materials in alkaline batteries [1,2]. Bivalent metal hydroxides such as nickel hydroxide, cobalt hydroxide and manganese hydroxide crystallize in brucite type structure, a mineral form of Mg(OH)<sub>2</sub>. The crystal structure of cobalt hydroxide comprises of a hexagonal close packing of hydroxyl ions in which alternate layer of octahedral sites are occupied by divalent Co<sup>2+</sup> ions. This results in the stacking of charge neutral layers with an interlayer distance of 4.6 Å [3,4].

Ismail et al. [5] proposed a common reaction mechanism for the reversible charge–discharge process in alkaline media:



Nickel hydroxide electrode exhibits step (a)/(d) reversibly with 1e<sup>−</sup> exchange, while nickel aluminium layered double hydroxide exhibits step (a and b)/(c and d) with 1.7e<sup>−</sup> exchange [6,7]. MnO<sub>2</sub> exhibits steps (b)/(c) reversibly, if the discharge is limited to 0.3e<sup>−</sup> exchange. Beyond this limit, Mn<sub>3</sub>O<sub>4</sub> spinel is formed [8]. Cobalt hydroxide can also exist in multiple oxidation states similar to nickel hydroxide [9]. Cobalt hydrox-

ide undergoes step (a) irreversibly resulting in the formation of an electrochemically inactive and highly resistive phase of HCoO<sub>2</sub>/CoOOH. While step (b)/(c) are quasi-reversibly cycled between the nearly quadrivalent (conducting) oxide phase and the insulating trivalent oxyhydroxide [10]. Cyclic voltammetric study of cobalt hydroxide thin films during cathodic sweep clearly shows the formation of Co<sub>3</sub>O<sub>4</sub> phase. Cyclic voltammetric studies of pure and doped cobalt hydroxide thin films with other divalent metals such as Mg<sup>2+</sup>, Ni<sup>2+</sup>, Zn<sup>2+</sup>, did not show any beneficial effect on the first step (a) of cobalt hydroxide [10]. Therefore, the full potential scheme for reversible charge storage capacity of cobalt hydroxide bulk electrode was not observed. The study of Co-base electro-active materials can provide useful information for the understanding of limiting phenomena affecting redox mechanism in layered materials.

Buss et al. overcome the limitation of irreversible behaviour of cobalt hydroxide by synthesizing cobalt aluminum and cobalt iron layered double hydroxide [11,12]. These layered double hydroxide electrodes reversibly exchange 0.4e<sup>−</sup>/Co. Wroblowa and Gupta blended small amount of Bi<sub>2</sub>O<sub>3</sub> with manganese oxide during electrode fabrication and succeeded in inducing 2e<sup>−</sup> exchange reversibility in manganese dioxide electrode [13]. Bi<sub>2</sub>O<sub>3</sub> coated cobalt hydroxide was used as additive to improve the electrochemical performance of nickel hydroxide electrode [14]. Bi<sub>2</sub>O<sub>3</sub> coated cobalt hydroxide suppress Co<sub>3</sub>O<sub>4</sub> formation during the charge–discharge process thereby increasing conductivity in the nickel hydroxide electrode. This clearly demonstrates that Bi<sub>2</sub>O<sub>3</sub> will suppress the spinel formation

\* Corresponding author. Tel.: +91 80 22961354.

E-mail address: [adityaramesh77@yahoo.com](mailto:adityaramesh77@yahoo.com) (T.N. Ramesh).

in cobalt hydroxide and manganese oxide electrodes during charge–discharge studies. The fundamental aspects behind the irreversible behaviour of cobalt hydroxide are not investigated. In this paper, we have studied the electrochemical behaviour of bulk cobalt hydroxide electrodes with and without  $\text{Bi}_2\text{O}_3$ .

## 2. Experimental

$\beta$ -Cobalt hydroxide and  $\text{Bi}_2\text{O}_3$  were obtained from Aldrich Chemical Co and Loba Chemie India and used as such. Bismuth doped cobalt hydroxides were also prepared by means of chemical precipitation. Simultaneous addition of mixed metal nitrates solution [ $\text{Co}(\text{NO}_3)_2$ : 0.9, 0.8 mol% and  $\text{Bi}(\text{NO}_3)_3$  0.1, 0.2 mol%] and  $\text{NaOH}$  (1 M) to a beaker containing an aqueous solution of sodium carbonate (0.5 M) results in the precipitation of the solid. The precipitation was stopped at pH at 9 and the product was aged in mother liquor at  $65^\circ\text{C}$  for 18 h prior to filtration [15]. The samples were filtered, washed with distilled water and dried at  $25\text{--}30^\circ\text{C}$  to constant weight.

The samples were characterized by powder X-ray diffraction (PXRD) using a Philips X'pert pro diffractometer (Cu  $\text{K}\alpha$  source,  $\lambda = 1.5418 \text{ \AA}$ ) with graphite as secondary monochromator.

### 2.1. Charge–discharge studies

Cyclic voltammetry studies (scan rate of  $10 \text{ mV s}^{-1}$ ) and galvanostatic charge discharge studies were carried out by Versastat Model II A (EG&G PARC) scanning potentiostat. Graphite powder was obtained from scientific chemicals (Chennai) and nickel foam was obtained from Nitech (thickness: 1.8 mm and porosity:  $500 \mu\text{m}$ ). Electrodes were prepared by mixing the active material with graphite powder and an aqueous suspension of poly-tetrafluoroethylene in the ratio 6:3:1. The mixtures were thoroughly ground to obtain a paste-like consistency in a pestle and mortar. This paste was pressed at  $75\text{--}120 \text{ kg cm}^{-2}$  on both sides of a nickel foam ( $2.9 \text{ cm} \times 2.3 \text{ cm}$ ) support at the ambient temperature  $25\text{--}30^\circ\text{C}$ .

Physically modified cobalt hydroxide electrodes were prepared by blending different ratios (2.5, 5, 10, 12 mol%) of  $\text{Bi}_2\text{O}_3$  with the active material. As prepared cobalt hydroxide– $\text{Bi}_2\text{O}_3$  composites was used as an active material during electrode fabrication. An electrode comprising  $\text{Bi}_2\text{O}_3$  without active material was also cycled to investigate its contribution to the charge storage capacity. All the electrodes were dried at  $65^\circ\text{C}$  and soaked in 6 M  $\text{KOH}$  for 24 h before being galvanostatically charged at current density of  $13 \text{ mA/cm}^2$  charged to 120% of the theoretical capacity computed for a  $1e^-$  exchange. The excess charge is to compensate for the side reactions such as oxygen evolution occurring during the charging process. Nickel plates were used as counters, and all potentials were measured using an  $\text{Hg/HgO/OH}^-$  reference electrode in 6 M  $\text{KOH}$ . These electrodes were then discharged at a current of 20 mA to a cutoff voltage of 0 V at the  $25\text{--}30^\circ\text{C}$ . The discharge current was chosen to yield a C/4 rate for the expected theoretical capacity of the electrode. The discharge capacities of all the electrodes were normalized with respect to the weight of the active material. After cycling

the electrodes were removed from the cell, rinsed with distilled water and dried at  $25\text{--}30^\circ\text{C}$  in a dessicator.

## 3. Results and discussion

Fig. 1a shows the PXRD pattern of cobalt hydroxide. The PXRD patterns display sharp Bragg reflections with  $d$ -values of 1.78, 2.38 and  $4.6 \text{ \AA}$ . The  $d$ -values match well with  $\beta$ -cobalt hydroxide (ICSD No. 88940). Cyclic voltammetric studies on cobalt hydroxide thin film exhibit two anodic peaks at 0.36,  $-0.64 \text{ V}$  and one cathodic peak at  $0.04 \text{ V}$  versus  $\text{Hg/HgO/OH}^-$ , respectively [10]. Anodic peak at  $0.36 \text{ V}$  is due to irreversible oxidation of  $\text{Co(II)}$  to  $\text{Co(III)}$  and the second quasi-reversible  $-0.64 \text{ V}$  peak is due to oxidation of  $\text{Co(III)}$  to  $\text{Co(IV)}$ . Cyclic voltammogram of bulk cobalt hydroxide is given in Fig. 2. Cobalt hydroxide bulk electrodes show peaks at  $0.33 \text{ mV}$  due

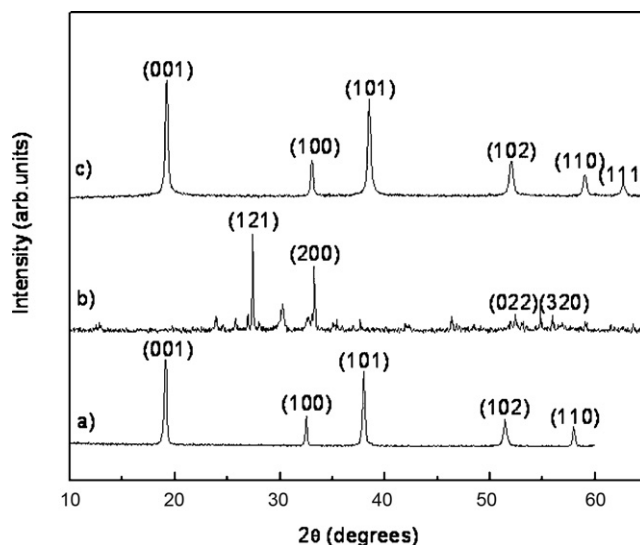


Fig. 1. PXRD patterns of (a) crystalline  $\beta$ -cobalt hydroxide, (b) commercial  $\text{Bi}_2\text{O}_3$  and (c) crystalline  $\beta$ -nickel hydroxide samples.

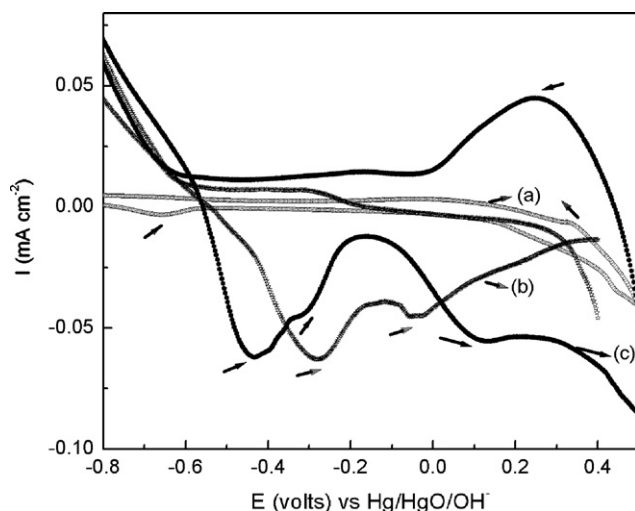


Fig. 2. Cyclic voltammogram of (a) cobalt hydroxide electrode, (b)  $\text{Bi}_2\text{O}_3$  and (c) 12 mol%  $\text{Bi}_2\text{O}_3$  blended cobalt hydroxide electrode at scan rate of  $10 \text{ mV/s}$ .

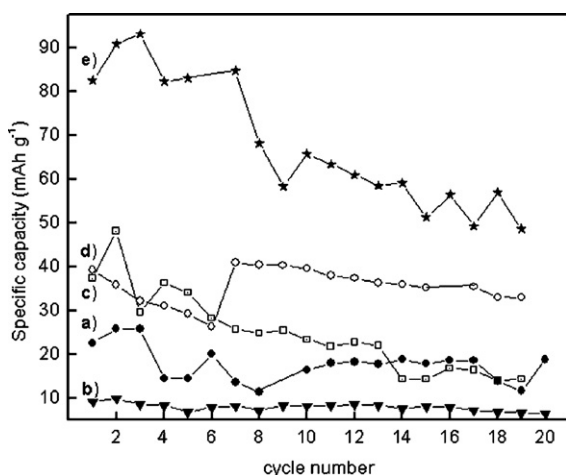


Fig. 3. Cycle life data of (a) cobalt hydroxide, (b)  $\text{Bi}_2\text{O}_3$ , cobalt hydroxide with (c) 2.5 mol%  $\text{Bi}_2\text{O}_3$ , (d) 5 mol%  $\text{Bi}_2\text{O}_3$  and (e) 12 mol%  $\text{Bi}_2\text{O}_3$ .

to oxidation of Co(II) to Co(III) and  $-0.65$  mV due to reduction of Co(IV) to Co(III). We have restricted our studies from Co(II) to Co(III) region, during which highly resistive CoOOH/ $\text{Co}_3\text{O}_4$  phase is formed.

Fig. 3a shows the cycle life data of cobalt hydroxide electrode and it exchanges  $0.1e^-/\text{Co}$ . Similar results was also observed by Elumalai et al. [16]. The discharge profile of cobalt hydroxide does not show plateau potential in the range of 450–0 mV (see Fig. 4a). The PXRD patterns of as-prepared fresh cobalt hydroxide, charged and discharged electrodes are shown in Fig. 5. On charging, cobalt hydroxide electrode gets oxidized to CoOOH. CoOOH also crystallizes in the layered structure similar to  $\beta$ -cobalt hydroxide. The absence of reflections in the PXRD pattern of charged state of cobalt hydroxide is due to the amorphous nature (see Fig. 5b). On discharge, we observe (i) peaks due to CoOOH,  $\text{Co}_3\text{O}_4$  and (ii) a less intense peak for cobalt hydroxide (see Fig. 5c). The PXRD patterns clearly show the structural changes that can take place during the charge discharge process of cobalt hydroxide. Cobalt hydroxide will also undergo oxi-

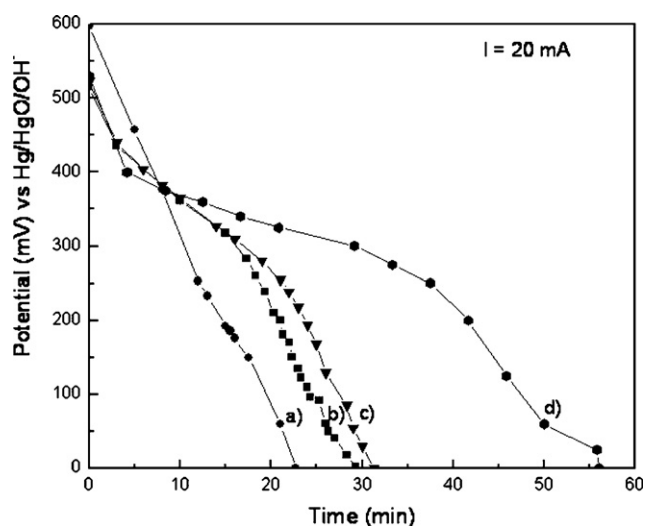


Fig. 4. Discharge profiles of (a) cobalt hydroxide, (b) with 2.5 mol%  $\text{Bi}_2\text{O}_3$ , (c) with 5 mol%  $\text{Bi}_2\text{O}_3$  and (d) with 12 mol%  $\text{Bi}_2\text{O}_3$ .

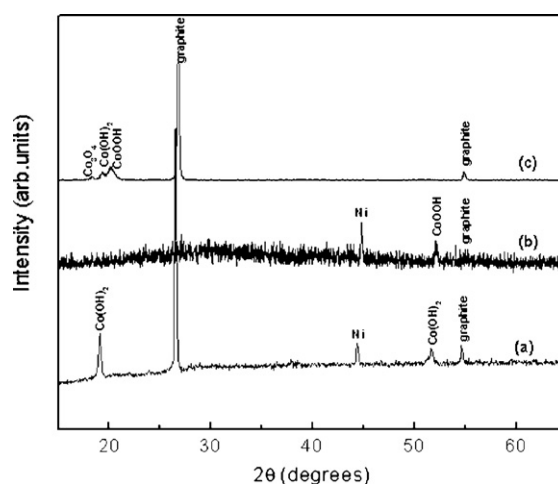


Fig. 5. PXRD patterns of (a) fresh cobalt hydroxide, (b) charged and (c) discharged cobalt hydroxide electrodes.

dation in KOH to form highly insulating phase of  $\text{Co}^{\text{III}}\text{OOH}$  [17];  $\text{Co}^{\text{III}}\text{OOH}$  further transforms to  $\text{Co}_3\text{O}_4$  [14,17]. This is the cause of an irreversible electrochemical behaviour in cobalt hydroxide.

In manganese dioxide, reversible electrochemical behaviour was achieved by two approaches [18]. In the first method, when the discharge of  $\text{MnO}_2 \rightleftharpoons \text{MnOOH}$  was limited to  $0.3e^-/\text{Mn}$  ( $\text{MnO}_2 \rightleftharpoons \text{Mn}_{1-x-y}^{4+}\text{Mn}_y^{3+}\text{O}_{2-4x-y}\text{O}^{2-}\text{OH}_{4x+y}^-$ ;  $y=0.3$ ) it can be reversibly cycled. In second method, Wroblowa and Gupta could reversibly cycle manganese dioxide [ $\text{MnO}_2 \rightleftharpoons \text{MnOOH} \rightleftharpoons \text{Mn}(\text{OH})_2$ ] upto  $2e^-$  exchange by incorporating small percentage of  $\text{Bi}_2\text{O}_3$ . The latter result is a direct evidence for the common reaction mechanism proposed by Ismail et al. [5]. Cyclic voltammogram study shows that  $\text{Bi}_2\text{O}_3$  doped manganese dioxide and  $\text{Bi}_2\text{O}_3$  coated cobalt hydroxide prevents  $\text{M}_3\text{O}_4$  ( $\text{M} = \text{Co}, \text{Mn}$ ) formation [14,19]. Several authors report the formation of Mn–Bi complexes in alkaline medium [19–21]. Pralong et al. soaked cobalt hydroxide in KOH solution containing bismuth nitrate. After 10 days, the product was recovered. The PXRD pattern of the recovered product does not show any trace of  $\text{Co}_3\text{O}_4$  formation [14]. The isostructural relationship between manganese dioxide and cobalt hydroxide promotes us to investigate the effect of  $\text{Bi}_2\text{O}_3$ , on cobalt hydroxide electrode from fundamental point of view.

Fig. 1b shows the PXRD pattern of commercial  $\text{Bi}_2\text{O}_3$ . The Bragg reflections in the PXRD pattern were indexed to  $\alpha$ -phase of  $\text{Bi}_2\text{O}_3$ . Cobalt hydroxide was physically mixed with various proportions of (2.5–12 mol%)  $\text{Bi}_2\text{O}_3$  during electrode fabrication. Cyclic voltammogram of  $\text{Bi}_2\text{O}_3$  is shown in Fig. 2b. We observe peaks at  $-0.54$ ,  $-278$  and  $-26$  mV due to reduction of  $\text{Bi}_2\text{O}_3$  to Bi. Cyclic voltammogram of 12 mol%  $\text{Bi}_2\text{O}_3$  modified cobalt hydroxide is shown in Fig. 2c. We observe peaks at 270 (due to the oxidation of cobalt hydroxide),  $-440$ ,  $-320$ ,  $-122$  (reduction of  $\text{Bi}_2\text{O}_3$  to Bi) and 125 mV (due to reduction of CoOOH), respectively. Cyclic voltammogram clearly shows that the presence of  $\text{Bi}_2\text{O}_3$  induces reversibility in cobalt hydroxide electrode. The cyclic voltammograms presented in this article are the representative profiles for the samples tested.

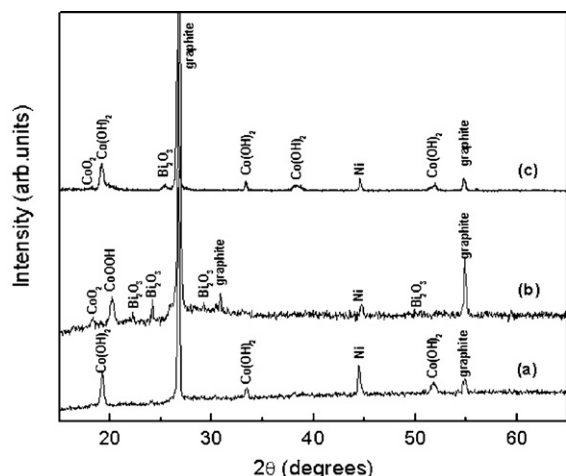


Fig. 6. PXR D patterns of (a) fresh  $\text{Bi}_2\text{O}_3$  modified cobalt hydroxide, (b) charged  $\text{Bi}_2\text{O}_3$  modified cobalt hydroxide and (c) discharged  $\text{Bi}_2\text{O}_3$  modified cobalt hydroxide.

Fig. 3a shows the cycle life data of plane cobalt hydroxide. In Fig. 3c–e is shown the cycle life data of cobalt hydroxide with 2.5, 5 and 12 mol% of  $\text{Bi}_2\text{O}_3$  (physically mixed), respectively. At 12 mol%  $\text{Bi}_2\text{O}_3$  addition (see Fig. 3e), cobalt hydroxide exchanges  $0.3\text{--}0.4e^-$ . Since the cutoff voltage during the discharge process in cobalt hydroxide is limited to 0 V, the reduction of  $\text{Bi}_2\text{O}_3$  to Bi is not feasible. In Fig. 4b–d are shown the discharge plateaus of cobalt hydroxide with 2.5, 5 and 12 mol%  $\text{Bi}_2\text{O}_3$ . The redox couple of  $\text{Co}^{3+}/\text{Co}^{2+}$  is expected to be in the range of 0.35–0.20 mV. 12 mol%  $\text{Bi}_2\text{O}_3$ , modified cobalt hydroxide shows a plateau in the range of 0.32–0.29 mV.

To further confirm that  $\text{Bi}_2\text{O}_3$  induces reversibility in cobalt hydroxide and does not get reduced during the course of the discharge process; we have recorded the PXR D patterns of 12 mol%  $\text{Bi}_2\text{O}_3$  modified cobalt hydroxide: (i) fresh electrode, (ii) on charging and (iii) after it was discharged (see Fig. 6a–c). On charging  $\text{Bi}_2\text{O}_3$  blended cobalt hydroxide, the electrode will display a peak at  $4.39 \text{ \AA}$  in the PXR D pattern due to the formation of  $\text{CoOOH}$  in addition to  $\text{Bi}_2\text{O}_3$  peaks (see Fig. 6b). On discharge, the  $d$ -value increases from  $4.39$  to  $4.6 \text{ \AA}$  due to the reduction of  $\text{CoOOH}$  to cobalt hydroxide ( $d = 4.6 \text{ \AA}$ ) (see Fig. 6c). The PXR D patterns of charged and discharged electrodes observed in Fig. 6 were recorded after 20 cycles. This clearly shows that  $\text{Bi}_2\text{O}_3$  induces reversibility in cobalt hydroxide without being reduced. Several authors have reported the cyclic voltammogram and show that the  $\text{Bi}_2\text{O}_3$  reduction takes place in the negative potential [14,19]. In order to rule out the possible contribution of  $\text{Bi}_2\text{O}_3$  in the positive potential window, we cycled  $\text{Bi}_2\text{O}_3$  bulk electrode and the cycle life data is shown in Fig. 3b. It exchanges less than  $0.1e^-/\text{Bi}_2\text{O}_3$ .

Layered double hydroxides derive their structure from magnesium hydroxide  $\text{Mg}(\text{OH})_2$ . Partial substitution of divalent metal ion by trivalent creates positive charge on the layer  $[\text{Mg}_{1-x}\text{Al}_x(\text{OH})_{2-x}]$ . To balance the positive charge on the layers, anions and water molecules get intercalated in the inter-layer region resulting in an increase in the inter lamellar spacing from  $4.6$  to  $7.6 \text{ \AA}$  [22]. Layered double hydroxides (Ni–Al,

Table 1

The  $d$ -values in the PXR D pattern of chemically prepared Co–Bi (Bi = 10 and 20 mol%) samples

Co–Bi (10 mol%)	$d$ ( $\text{\AA}$ )	Co–Bi (20 mol%)	$d$ ( $\text{\AA}$ )
(003)	6.99	(003)	6.99
(006)	3.67	(001) <sup>a</sup>	4.63
(012)	2.94	(006)	3.67
(015)	2.70	(012)	2.98
–	2.12	(015)	2.70
$\text{Bi}_2\text{O}_3$	1.86	(101) <sup>a</sup>	2.36
$\text{Bi}_2\text{O}_3$	1.76	$\text{Bi}_2\text{O}_3$	1.90
$\text{Bi}_2\text{O}_3$	1.69	$\text{Bi}_2\text{O}_3$	1.76
$\text{Bi}_2\text{O}_3$	1.66	$\text{Bi}_2\text{O}_3$	1.60
$\text{Bi}_2\text{O}_3$	1.60		

<sup>a</sup> Peaks due to  $\beta$ -cobalt hydroxide.

Ni–Co, Ni–Mn, Ni–Zn) are extensively used as electrode materials and are known to perform better than nickel hydroxide electrodes [7,23–25]. Our attempt to prepare Co–Bi layered double hydroxides  $[\text{Co}_{1-x}\text{Bi}_x(\text{OH})_{2-y}(\text{A}_y)^{n-} \cdot z\text{H}_2\text{O}]$  where  $x = 0.1$  and  $0.2$ ] failed, since the ionic radii of Bi is larger than the octahedral void present within the layer. The Bragg reflections in the PXR D pattern of chemically prepared Co–Bi (10 and 20 mol%) compounds could be indexed to mixture of Co–Bi layered double hydroxide,  $\beta$ -cobalt hydroxide and  $\text{Bi}_2\text{O}_3$  (see Table 1). The cycle life data of 10 and 20 mol% chemically prepared  $\text{Bi}_2\text{O}_3$  doped cobalt hydroxide are shown in Fig. 7b and c. In Fig. 8a and b are shown the discharge plateaus of 10 and 20 mol% of chemically prepared  $\text{Bi}_2\text{O}_3$  cobalt hydroxide. Chemically modified cobalt hydroxide with  $\text{Bi}_2\text{O}_3$  shows slightly higher reversible discharge capacity ( $0.5e^-/\text{Co}$ ) compared to physical mixture due to the formation of Co–Bi layered double hydroxide and intimate mixing of cobalt hydroxide and  $\text{Bi}_2\text{O}_3$  during precipitation. Solid solution of cobalt substituted nickel hydroxide obtained by co precipitation performs electrochemically better than the nickel hydroxide with post treat of

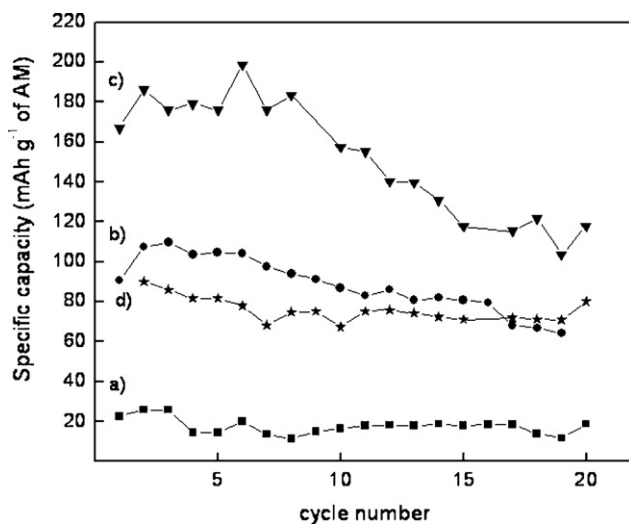


Fig. 7. Cycle life data of (a) cobalt hydroxide, (b) 10 mol% bismuth doped cobalt hydroxide, (c) 20 mol% bismuth doped cobalt hydroxide and (d) crystalline  $\beta$ -nickel hydroxide electrodes.



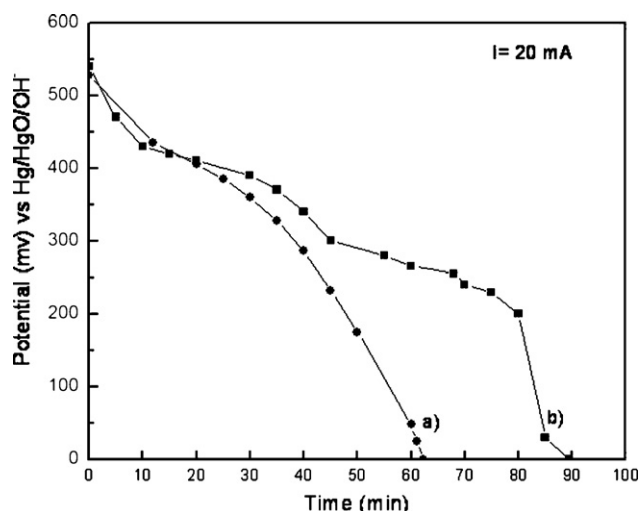


Fig. 8. Discharge profiles of (a) 10 mol% bismuth doped cobalt hydroxide and (b) 20 mol% bismuth doped cobalt hydroxide, respectively.

cobalt [26]. Several studies concerning relationship between the insertion/substitution of Co by other transition elements and the structural/conductivity properties of Co oxides have been previously reported [27]. Pralong et al. show that, highly conducting phase of  $\text{Co}_x^{4+}\text{Co}_{1-x}^{3+}\text{OOH}_{1-x}$  phase is formed in the presence of Bi [14].

The amphoteric nature of cobalt hydroxide leads to a dissolution in alkaline medium resulting in the shedding of the material.  $\text{Bi}_2\text{O}_3$  modified cobalt hydroxide to some extent prevents the dissolution of cobalt hydroxide. The surface area of cobalt hydroxide and chemically prepared  $\text{Bi}_2\text{O}_3$  modified cobalt hydroxide are given in Table 2.

In Fig. 1c is shown the PXRD pattern of crystalline  $\beta$ -nickel hydroxide. In case of nickel hydroxide, crystalline samples deliver very low discharge capacity compared to disordered samples [28]. In Fig. 7d is shown the cycle life data of crystalline  $\beta$ -nickel hydroxide which exchanges  $0.3e^-/\text{Ni}$ . Disordered samples show better electrochemical activity and the discharge capacity is close to the theoretical expected value [29]. Crystalline cobalt hydroxide (see Fig. 7a) also delivers low discharge capacity but the disordered form of cobalt hydroxide does not exist. Addition of nickel nitrate to strong alkali produces highly disordered material [28] whereas in case of cobalt system, use of strong alkali results in the oxidation of  $\text{Co}^{2+}$  to  $\text{Co}^{3+}$ . Weak base such as ammonia, precipitates  $\alpha$ -cobalt hydroxide, which immediately transforms into crystalline phase of  $\beta$ -cobalt hydroxide [30]. Hence, we get either biphasic mixture or highly ordered cobalt hydroxide. Therefore, disordered phase of  $\beta$ -cobalt hydroxide is not reported.

Table 2  
BET surface area measurements

Sample	Surface area ( $\text{m}^2 \text{g}^{-1}$ )
$\beta$ -Cobalt hydroxide	16.9
Co–Bi (20 mol%) composite	19.3

#### 4. Conclusion

Cobalt hydroxide electrode exchanges  $0.1e^-$  while  $\text{Bi}_2\text{O}_3$  modified cobalt hydroxide electrode (chemically and physically) reversibly exchanges  $0.3\text{--}0.5e^-$ .  $\text{Bi}_2\text{O}_3$  prevents the  $\text{Co}_3\text{O}_4$  formation in cobalt hydroxide during the charge–discharge process. We demonstrate that  $\text{Bi}_2\text{O}_3$  modified cobalt hydroxide induces reversibility providing some insights into the charge discharge process of cobalt hydroxide.

#### Acknowledgments

T.N.R. thanks the Council of Scientific and Industrial Research, GOI for the award of a Senior Research Fellowship (NET) and Research Associate (RA). P.V.K. thanks the Department of Science and technology, Government of India (GOI) for financial support. Authors thank the Solid State and Structural Chemistry Unit, Indian Institute of Science for powder X-ray diffraction facilities. Authors thank anonymous referees for their useful comments.

#### References

- [1] S.U. Falk, A.J. Salkind, *Alkaline Storage Batteries*, Wiley, New York, 1969.
- [2] K. Kordes, M. Weissenbacher, *J. Power Sources* 51 (1994) 61.
- [3] A.F. Wells, *Structural Inorganic Chemistry*, Oxford University Press, Oxford, 1979.
- [4] H.R. Oswald, R. Asper, in: R.M.A. Lieth (Ed.), *Preparation and Crystal Growth of Materials with Layered Structures*, vol. 1, D. Reidel Publishing Company, Holland, 1977, p. 71.
- [5] J. Ismail, M.F. Ahmed, P.V. Kamath, *J. Power Sources* 36 (1991) 507.
- [6] H. Bode, K. Dehmelt, J. Witte, *Electrochim. Acta* 11 (1966) 1079.
- [7] P.V. Kamath, M. Dixit, L. Indira, A.K. Shukla, V.G. Kumar, N. Munichandraiah, *J. Electrochem. Soc.* 141 (1994) 2956.
- [8] J. McBreen, in: D.H. Collins (Ed.), *Power Sources*, vol. 5, Academic Press, London, 1975, p. 31.
- [9] M. Figlarz, J. Guenot, J.-N. Tournemolle, *J. Mater. Sci.* 9 (1974) 772.
- [10] J. Ismail, M.F. Ahmed, P.V. Kamath, *J. Power Sources* 41 (1993) 223.
- [11] D.H. Buss, J. Bauer, W. Diembeck, O. Glemser, *J. Chem. Soc. Chem. Commun.* 2 (1985) 81.
- [12] J. Bauer, D.H. Buss, H.-J. Harms, O. Glemser, *J. Electrochem. Soc.* 137 (1990) 173.
- [13] H.S. Wroblowa, N. Gupta, *J. Electroanal. Chem.* 238 (1987) 93.
- [14] V. Pralong, A. Delahaye-Vidal, B. Beaudoin, J.-B. Leriche, J. Scoyer, J.-M. Tarascon, *J. Electrochem. Soc.* 147 (2000) 2096.
- [15] W.T. Reichle, *J. Catal.* 941 (1985) 547.
- [16] P. Elumalai, H.N. Vasan, N. Munichandraiah, *J. Power Sources* 93 (2001) 201.
- [17] V. Pralong, A. Delahaye-Vidal, B. Beaudoin, B. Gerand, J.-M. Tarascon, *J. Mater. Chem.* 9 (1999) 955.
- [18] D. Im, A. Manthiram, *J. Electrochem. Soc.* 150 (2003) A68.
- [19] C.G. Castledine, B.E. Conway, *J. Appl. Electrochem.* 25 (1995) 707.
- [20] M. Bodé, C. Cachet, S. Bach, J.-P. Pereira-Ramos, J.C. Ginoux, L.T. Yu, *J. Electrochem. Soc.* 144 (1997) 792.
- [21] L.T. Yu, *J. Electrochem. Soc.* 144 (1997) 802.
- [22] F. Cavani, F. Trifiro, A. Vaccari, *Catal. Today* 11 (1991) 173.
- [23] C. Delmas, C. Faure, Y. Borthomieu, *Mater. Sci. Eng. B13* (1992) 89.
- [24] L. Demourgues-Guerlou, C. Denage, C. Delmas, *J. Power Sources* 52 (1994) 269.

- [25] M. Dixit, P.V. Kamath, J. Gopalakrishnan, *J. Electrochem. Soc.* 146 (1999) 79.
- [26] X. Li, T. Xia, H. Dong, Y. Wei, *Mater. Chem. Phys.* 100 (2006) 486.
- [27] F. Tronel, L. Guerlou-Demourgues, M. Menetrier, L. Croguennec, L. Goubault, P. Bernard, C. Delmas, *Chem. Mater.* 18 (2006) 5840.
- [28] R.S. Jayashree, P.V. Kamath, G.N. Subbanna, *J. Electrochem. Soc.* 147 (2000) 2029.
- [29] T.N. Ramesh, P.V. Kamath, C. Shivakumara, *J. Electrochem. Soc.* 152 (2005) 806.
- [30] Z.P. Xu, H.C. Zeng, *Chem. Mater.* 11 (1999) 67.